Yamada K, Green KG, Samarel AM, Saffitz JE (2005) Distinct pathways regulate expression of cardiac electrical and mechanical junction proteins in response to stretch. Circ Res 97:346–353

Yokomori H, Oda M, Yoshimura K, Nagai T, Ogi M, Nomura M, Ishii H (2003) Vascular endothelial growth factor increases fenestral permeability in hepatic sinusoidal endothelial cells. Liver Int 23:467–475

Yokomori H, Yoshimura K, Funakoshi S, Nagai T, Fujimaki K, Nomura M, Ishii H, Oda M (2004) Rho modulates hepatic sinusoidal endothelial fenestrae via regulation of the actin cytoskeleton in rat endothelial cells. Lab Invest 84:857–864

Zahler S, Hoffmann A, Gloe T, Pohl U (2003) Gap-junctional coupling between neutrophils and endothelial cells: a novel modulator of transendothelial migration. J Leukoc Biol 73:118–126

A Novel Method for Three-Dimensional Observation of the Vascular Networks in the Whole Mouse Brain

HISASHI HASHIMOTO,[1]* MORIAKI KUSAKABE,[2,3] AND HIROSHI ISHIKAWA[1]
[1]*Department of Anatomy, The Jikei University School of Medicine, Minatoku, Tokyo 105-8461, Japan*
[2]*Institute for Animal Reproduction, Experimental Animal Research Center, Ibaraki 300-0134, Japan*
[3]*Matrix Cell Research Institute, Inc, Ibaraki 300-0134, Japan*

KEY WORDS three-dimensional image; blood vessels; brain; mouse; paraffin

ABSTRACT A novel method for acquiring serial images suitable for three-dimensional reconstruction of vascular networks in the whole brain of mouse was developed. The brain infused with a White India ink-gelatin solution was fixed and embedded in paraffin containing Sudan Black B through xylene also containing Sudan Black B. Each sliced surface of the paraffin block was coated with liquid paraffin and its image was serially acquired. Coating with liquid paraffin extremely improved the quality of the image. The series of serial images was free of distortion and a three-dimensional image was reconstructed without the problem of the alignment and registration of adjacent images. The volume-rendered image indicated three-dimensional distribution of blood vessels in a whole brain. No ghost or shadow was observed on a volume-rendered image of the White India ink-gelatin infused brain. The *z*-axial resolution examined on the orthogonal sections reconstituted from serial images obtained at an interval of 5 μm showed no cross talk, indicating that the *z*-axial resolution was no larger than 5 μm. A proper understanding of the vascular system in a whole brain is indispensable to reveal the development of the vascular system in the brain of normal and genetically manipulated mouse and vascular alterations in pathological situation, such as stroke and neurodegenerative disease. Although simple and inexpensive, this method will provide fundamental information on the vascular system in a whole brain. *Microsc. Res. Tech. 71:51–59, 2008.*

INTRODUCTION

Three-dimensional observation of the biological object is effective and essential to a proper understanding its structure. The confocal laser scanning microscope (CLSM) has become popular in recent years and made it possible to observe three-dimensional structures of a thick object. A series of serial images is easily obtained by optical sectioning of the thick object with CLSM and is easily reconstructed into three-dimensional images. However, an application of confocal laser scanning microscopy has some week points, such as a limitation on the thickness of the specimen and low axial resolution.

Three-dimensional distribution of blood vessels in the brain of the mouse and the rat has widely studied on a thick section of the brain infused with Indian ink or fluorochrome-labeled gelatin, and on a corrosion cast of vessels in the brain (Coyle, 1975, 1978; Coyle and Jokelainen, 1982; Hashimoto et al., 1998b; Hashimoto et al., 1999; He et al., 2000; Koppel 1982; Rieke, 1987; Rieke et al., 1981; Scremin, 2004; Ward et al., 1990). However, manual manipulation of the focusing plan of a microscope is required to reveal the three-dimensional distribution of blood vessels in a thick section of the Indian ink infused brain. Scanning electron microscopy can produce two-dimensional images of the surface of the corrosion cast of blood vessels from various viewpoints and provide a three-dimensional appearance, though the superficial casts must be removed to observe the deeper vessels. The CLSM observation of a fluorochrome-labeled gelatin infused specimen can provide a series of serial images by optical sectioning and a real three-dimensional image of the blood vessels can be produced only in a limited depth. In the last decade, a microcomputer tomography (μCT) has been developed and applied to the observation of vascular networks (Bentley et al., 2002; Jorgensen et al., 1998; Krucker et al., 2006) and, furthermore, synchrotron radiation μCT was introduced (Plouraboué et al., 2004). The recent development and advances in synchrotron radiation μCT technologies enabled to observe the three-dimensional distribution of the vascular networks at increasing levels of resolution (Heinzer et al., 2006). However, the μCT is not generally available yet.

To make a three-dimensionally reconstructed image of a comparatively large specimen, such as a vascular networks in a whole mouse brain, serial sectioning may be the only way to be adopted. However, the problem of the distortion of a section and the difficulties in fitting the position of adjacent sections are inevitable to reconstruct a three-dimensional image from serial sections. In this study, we have tried to acquire serial

*Correspondence to: Hisashi Hashimoto, Department of Anatomy, The Jikei University School of Medicine, 3-25-8 Nishishinbashi, Minatoku, Tokyo 105-8461, Japan. E-mail: hashimoto.anat@jikei.ac.jp

H. Ishikawa is currently at the Laboratory of Regenerative Medical Science, The Nippon Dental University School of Life Dentistry at Tokyo, 1-9-20, Fujimi, Chiyoda-ku, Tokyo 102-8159, Japan.

Received 9 April 2007; accepted in revised form 2 August 2007

DOI 10.1002/jemt.20522

Published online 14 September 2007 in Wiley InterScience (www.interscience.wiley.com).

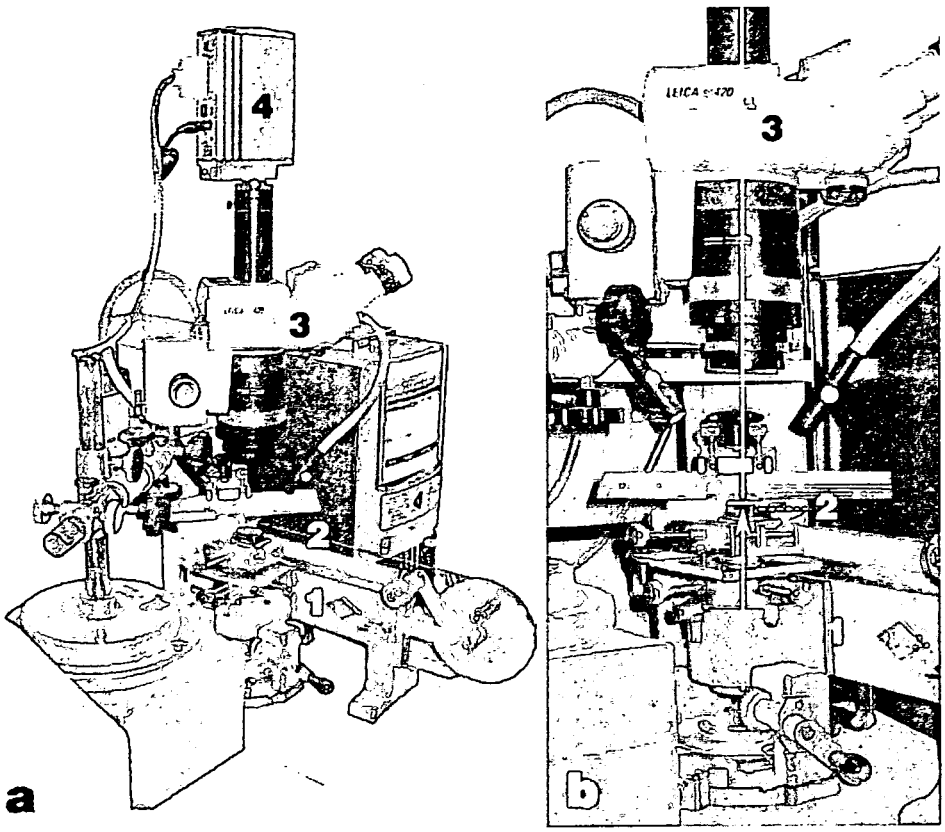

Fig. 1. Image acquisition system. An overview of our system (a) and a close-up around the stage of the microtome (b). The elevating axis of the stage (white arrow) is adjusted to the optical axis (white line) of the macroscope (b). (1) Heidelberg type sliding microtome. (2) paraffin block. (3) Leica M-420 macroscope equipped with an Apozoom lens. (4) Polaroid PDMC le digital camera.

images of vascular networks in a whole mouse brain with a novel method. In this method, a White India ink-gelatin solution was used to infuse vascular networks instead of an India ink-gelatin solution, and the specimen was embedded in paraffin containing Sudan Black B. Each sliced surface of the paraffin block was coated with liquid paraffin and its image was serially taken. The series of serial images was free of distortion and was able to reconstruct a three-dimensional image without the problem of the alignment and registration of adjacent images.

MATERIALS AND METHODS

Animals

Adult female mice of the BALB/cA strain kept in our laboratory were used in this study. Housing and preparations of mice was in accordance with institutional guidelines.

Preparation of Ink-Gelatin Solution

Two types of ink-gelatin solution were used. One was an India ink-5% gelatin solution (black) and the other was a White India ink-5% gelatin solution (white). The India ink is an aqueous solution of gelatinous colloid of carbon and the White India ink is an aqueous solution of gelatinous colloid of titanium oxide. Ten percent gelatin solution was prepared by swelling 4 g of gelatin (Gelatin RR, AIVIS, Tokyo, Japan) in 30 mL of water at 37°C, dissolving completely at 60°C and adding water to make a total volume of 40 mL. The 10% gelatin solution was kept dissolved in a warm water bath at 37°C and equal volume of the 10% gelatin solution and an India ink solution (Boku-jyu BO-1001, Kaimei, Saitama, Japan) were well mixed to make an India ink-5% gelatin solution. In the same manner, equal volume of the 10% gelatin solution and a White India ink solution (Hakuboku BO-8101, Kaimei) were well mixed to make a White India ink-5% gelatin solution.

Infusion With a Ink-Gelatin Solution

The ink-gelatin solution was loaded into a 5-mL syringe connected with a polyethylene needle via a plastic tube. The syringe with plastic tube and needle was kept at 37°C in a warm-water bath until use. The mice received intraperitoneal injection of an overdose of sodium pentobarbital solution. Under deep anesthesia, thoracotomy was performed. The heart was exposed and the thoracic aorta and vena cava inferior were clamped. The right atrium was injured to drain blood and then the mice were perfused from the left ventricle with 5 mL of phosphate buffered saline (PBS, pH 7.2), 10 mL of 10% buffered formalin solution and finally with 10 mL of PBS. After perfusion, a slit was made in the wall of the left ventricle and the polyethylene needle was inserted from the slit up to the ascending aorta, and then 3 mL of the ink-gelatin solution was slowly infused. After infusion, the ascending aorta and vena cava superior were clamped and the mice were immersed in crashed ice to make the ink-gelatin solution gel. After the ink-gelatin solution gelled, the whole brain was carefully removed and further fixed in 10% buffered formalin solution at 4°C for more than 1 week.

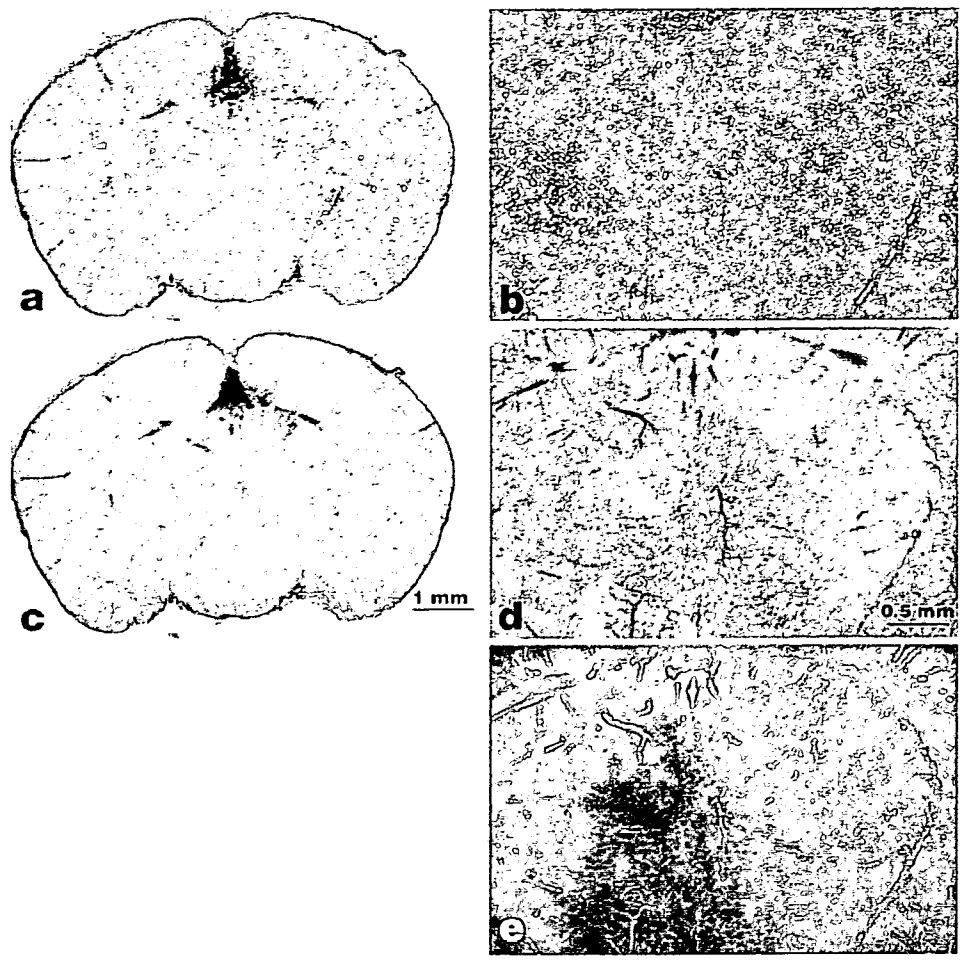

Fig. 2. Surface images of a paraffin block of an Indian ink-gelatin infused brain. Images of a newly cut surface were acquired before (a and b) and after (c and d) coating with liquid paraffin. Gray scale of image d was inverted (e). Coronal sections of a whole mouse brain (a and c) and magnified views (b and d) of diencephalon in a and c. The surface of a newly cut paraffin block is microscopically rough and vessels filled with India ink-gelatin are scarcely recognizable because of a diffused light (a and b). The surface image of liquid paraffin coated paraffin block are clear and sharp (c and d). Capillary networks filled with India ink-gelatin are detectable (d). The gray scale inverted image looks like a fluorescent image (e).

Paraffin Embedding

The India ink-gelatin infused brain was rinsed with water, dehydrated through an ascending series of ethanol and embedded in paraffin through xylene as usual.

The White India ink-gelatin infused brain was rinsed with water, immersed in a warm 1% aqueous agarose solution and the agarose solution was made to gel on ice. The brain in the agarose gel was dehydrated through an ascending series of ethanol and immersed in xylene two times. The brain was, then, immersed in xylene containing 0.1% (wt/vol) of Sudan Black B (192-044121 Wako Pure Chemical Industries, Osaka, Japan) for 2 days, in paraffin-saturated xylene containing 0.1% of Sudan Black B at 45°C, and in three changes of melted paraffin containing 0.1% of Sudan Black B (hereafter designated as the black paraffin) at 60°C, and embedded in the black paraffin.

Image Acquisition

The paraffin block was set on the stage of a Heidelberg type sliding microtome (R. Jung AG, Heidelberg, Germany). A Leica M-420 macroscope (equipped with an Apozoom objective lens 1:6, n.a. = 0.116, Leica Microsystems GmbH, Wetzlar, Germany) with a Polaroid PDMC Ie digital camera (Polaroid, MA) was placed above the microtome (Fig. 1a). The optical axis of the macroscope was adjusted to the elevating axis of the stage of the microtome (Fig. 1b). The macroscope was focused on a newly cut surface of the paraffin block and the built-in aperture diaphragm was set open to make the resolution higher and the depth of field narrower. The newly cut surface of the paraffin block was coated with a few drops of liquid paraffin (164-00476 Wako Pure Chemical Industries), and then a 16 bit gray-scale image of the surface was immediately acquired at 1,600 × 1,200 pixels with episcopic illumination. The stage was elevated by a step and the sample was sliced to expose a new surface. The new surface was coated with liquid paraffin and its image was acquired. These processes were repeated to obtain a complete set of serial images of the brain. The step employed was 5–20 μm.

Three Dimensional Reconstruction

The 16 bit gray-scale of the images of the India ink-gelatin infused brain was inverted to make the background black. The brightness and contrast of the image was adjusted to enhance the white vascular image against the black background and 16 bit gray-scale was downsized to 8 bit gray-scale. The periphery of the image, where no brain exited, was clipped off or

blacked out. The image size was reduced if necessary to reconstruct three-dimensional images. The images obtained from the White India ink-gelatin infused brain was also processed as well except gray-scale inversion. These image processings were performed with an Adobe Photoshop ver. 7.0 software (Adobe Systems, CA). Three-dimensional reconstruction was performed with an Imaris 4.2 volume rendering software (Bitplane AG, Zurich, Switzerland), some stereo pair images were obtained with a LSM dummy software (Carl Zeiss AG, Jena, Germany) and orthogonal section images with a LSM 5 image browser software (Carl Zeiss AG).

RESULTS

Effect of Liquid Paraffin on the Image Quality

The effect of liquid paraffin coating was examined on the image of the India-ink infused brain embedded in paraffin. However sharp the edge of a blade was, a bare newly cut surface of the paraffin block was microscopically rough. The image obtained from the surface was gritty, and even large vessels were barely recognizable though they had been filled with the Indian-ink gelatin (Figs. 2a and 2b). Coating with liquid paraffin extremely improved the quality of the image of the surface (Figs. 2c and 2d). Lots of vessels and even capillary networks were recognized in a higher magnified image (Figs. 2c and 2d). Portions of large vessels running deep in the paraffin block were also vaguely indicated and caused a false image (Fig. 2d). The gray scale of each image was inverted for three-dimensional image processing (Fig. 2e).

Three Dimensional Reconstruction of the India Ink-Gelatin Infused Brain

The India ink-gelatin infused brain was sliced and an image of each surface was acquired after coating with liquid paraffin. In a case of coronally slicing at a step of 10 μm, 1,000 complete serial images were obtained. A part of the serial images was taken out and stereo pair images viewed from *z*-direction were produced (Figs. 3a–3e). In these stereo pair images, three-dimensional distributions of blood vessels in a part of the brain were clearly indicated.

Volume-rendered images were obtained from complete serial images by the maximum intensity projection. These images indicated three-dimensional distribution of blood vessels in a whole brain (Figs. 4a–4f). However, shadows or ghosts of vessels on *z*-direction, derived from the false image of the vessels located in the deeper region, deteriorated the image quality. On the orthogonal sections, the length of the shadows extended over 1 mm and their intensity gradually declined (Figs. 4g and 4h). These shadows were obstructive to the observation of the volume-rendered image by the ray tracing method (not shown).

Three Dimensional Reconstruction of the White India Ink-Gelatin Infused Brain

The opaque paraffin was developed by dissolving the black pigment, Sudan Black B for lipid staining, into the melted paraffin, to eliminate the false image of vessels. Sudan Black B has easily dissolved in melted paraffin and also in xylene. In this study, we designate black-colored xylene and black-colored paraffin as

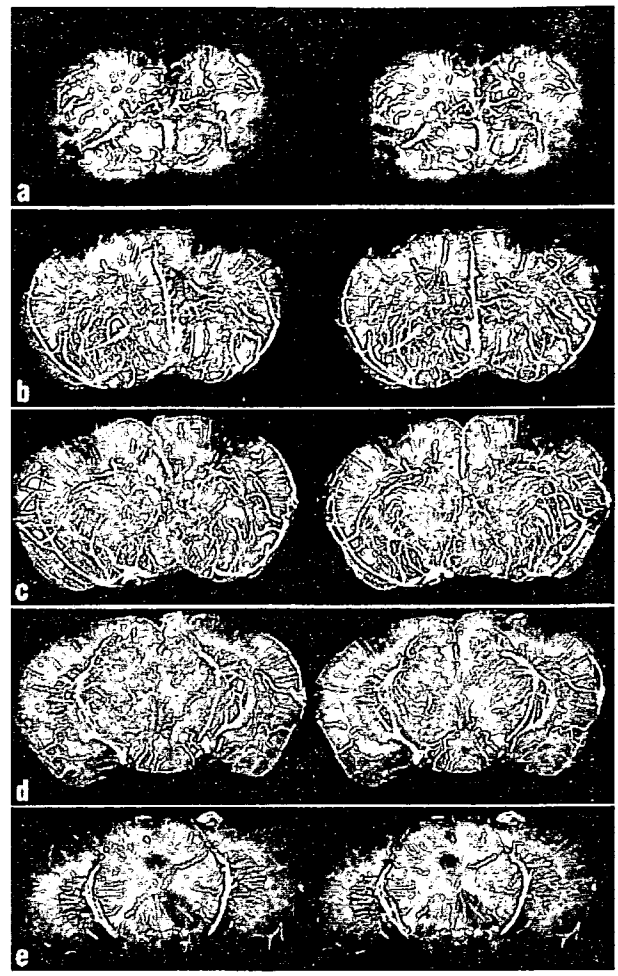

Fig. 3. Stereo pair images of an India ink-gelatin infused brain. A total of 1,000 coronal sections at an interval of 10 μm were acquired from an India ink-gelatin infused mouse brain. Stereo pair images were obtained from a part of serial sections with a LSM dummy software. Stereo pair images reconstructed with 150 serial images, 1st–150th image (a) and 151st–300th image (b), and with 200 serial images, 301st–500th image (c), 451st–650th image (d) and 601st to 800th image (e). A part of a three-dimensional distribution of blood vessels is clearly displayed in stereo pair images.

black xylene and black paraffin, respectively. The black xylene and black paraffin easily penetrated into a dehydrated mouse brain and stained the brain black, forming a striking contrast with blood vessels filled with the White India ink-gelatin. While the surface image of black paraffin itself was not homogeneous but spotty, that of agarose and the brain in black paraffin was very smooth and homogeneous (Fig. 5a). Furthermore, agarose used to embed the brain played a role of a guide to find the brain in black paraffin.

The White India ink-gelatin infused brain was sliced and an image of each surface was acquired after coating with liquid paraffin. In case of a horizontally slicing at a step of 5 μm, 1,000 complete serial images were obtained. The volume-rendered image obtained by the maximum intensity projection or by the ray tracing method clearly indicated three-dimensional distribu-

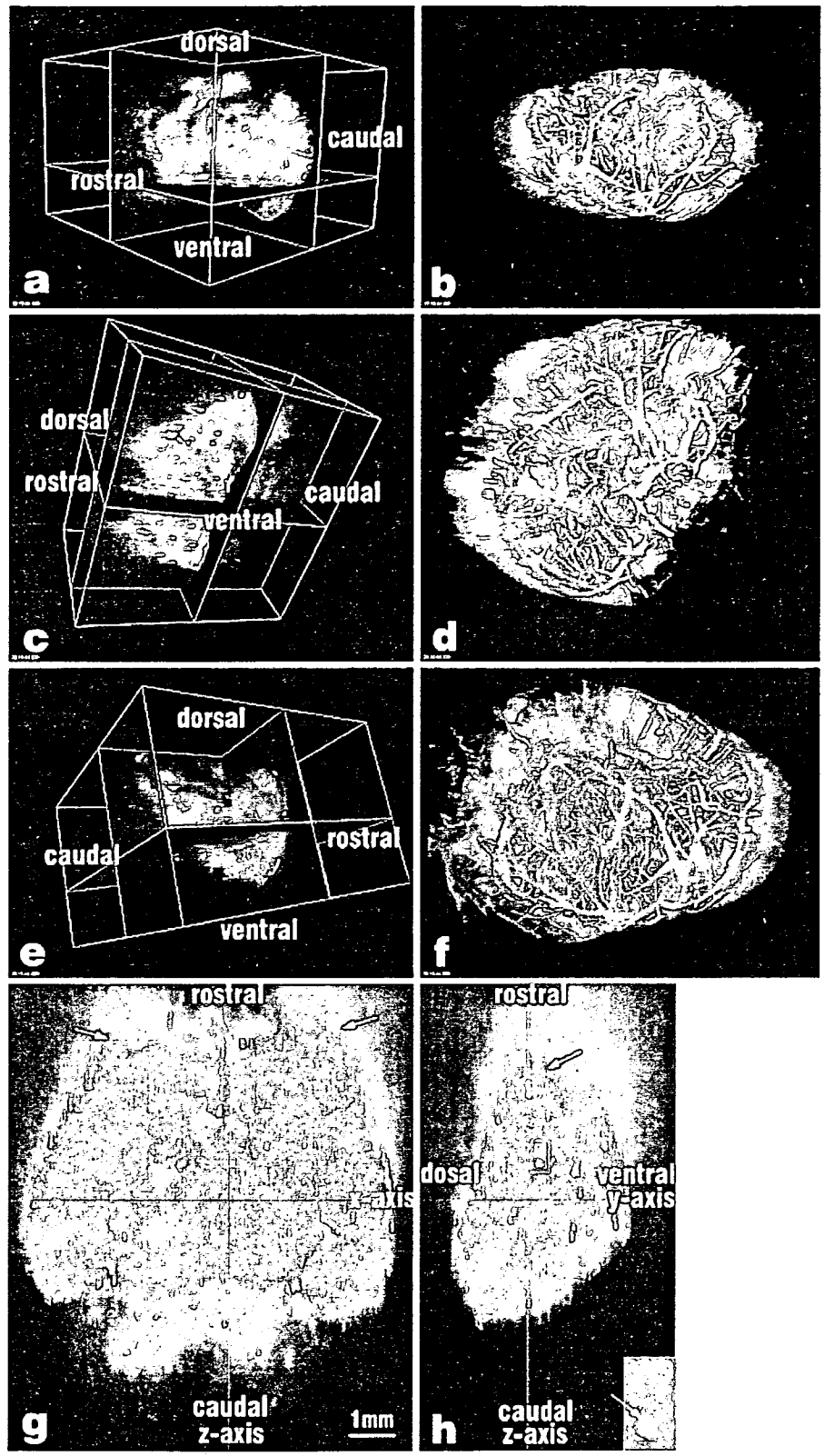

Fig. 4. Three-dimensional reconstruction of a series of serial sections from an India ink-gelatin infused brain. A total of 1,000 coronal sections at an interval of 10 μm were acquired from an India ink-gelatin infused mouse brain. Alternate sections were picked up and the image size was reduced by 50%, because of the limitation of the hardware. Then, three-dimensional reconstruction was performed with an Imaris 4.2 (a–f). Spatial orientation is indicated (**a**, **c**, and **e**). Volume-rendered images by the maximal intensity projection (**b**, **d**, and **f**). Orthogonal section images on *y*-axis (**g**) and *x*-axis (**h**) were obtained with a LSM 5 image browser software. Inset in h is a magnified view of a rectangular area indicated with white lines. Once serial sections are imported into a volume rendering software, three-dimensional images from various view points are easily calculated. Three-dimensional distribution of blood vessels in a whole mouse brain is readily observed, but ghosts or shadows of vessels interfere with observation (b, d, and f). Orthogonal section images indicate that shadows or ghosts (white arrows) extends over 1 mm (g and h).

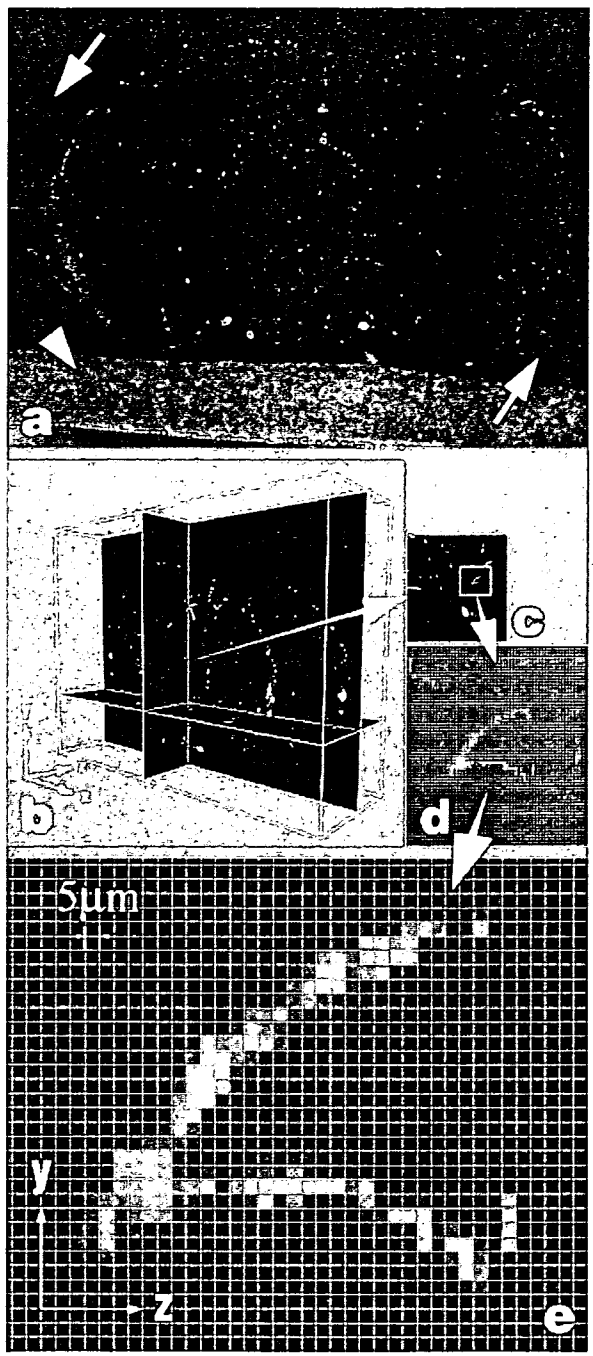

Fig. 5. Images of a White India ink-gelatin infused brain. An image of a coronally cut surface of a White India ink-gelatin infused brain (a). Orthogonal section image on x-axis and its magnified images (b, c, d, and e). Orthogonal section image on x-axis (b and c) was obtained from 150 coronal serial sections obtained at an interval of 5 μm and a part of the image was enlarged (d and e). While the image of the surface of black paraffin alone is rough and looks sandy (white arrow head in a), that of agarose is as smooth as that of the brain (white arrows in a). On the orthogonal section image and its enlarged images, no ghost or shadow is seen (c, d and e). Each square enclosed with white lines indicates a pixel and each vertical column of squares indicate a cross section of the original coronal section image (e). This enlarged image reveals that the resolution along the z-axis is lower than 5 μm.

tion of blood vessels in a whole brain (Figs. 6a–6i and 7). No ghost or shadow was observed on the three-dimensionally reconstructed images and also on the orthogonal sections (Figs. 5b–5e, 6a–6i, and 7). The z-axial resolution was examined on the orthogonal sections reconstituted from serial images obtained at a step of 5 μm and no overlap or cross talk was found, indicating that the z-axial resolution was no larger than 5 μm (Figs. 5b–5e). Two types of noise, however, were found on the volume-rendered image (Figs. 6 and 7). One was sporadic spots of various sizes and located throughout the image. The other was fine straight lines parallel to the z-axis extending from the first image plane to the last one. Both types of noise appeared as white spots on each surface image and were difficult to be distinguished from signals of the White India ink in vessels. Some major arteries found on a volume-rendered image by the ray tracing method were named in Figure 7. Anyway, it was possible to observe three-dimensionally the distribution of blood vessels in a whole mouse brain from any direction and on any magnification.

DISCUSSION

The present study indicated a novel method for three-dimensional observation of vascular networks in a whole mouse brain. In this method, the White India ink-gelatin solution was used to infuse the blood vessels of a brain, and the brain was embedded in black paraffin. A series of serial images of vascular networks in the brain was obtained from each newly sliced surface of the paraffin block after coating with liquid paraffin, and three-dimensional images were reconstructed from them. The volume-rendered image of the White India ink-gelatin infused brain clearly indicated the three-dimensional distribution of vascular networks in the whole mouse brain.

In our method, an image of each newly sliced surface of the paraffin block was acquired, not from the bare surface, but from the surface after coated with liquid paraffin. Bare sliced surface images have been taken in some projects. The collection of sliced surface images of a frozen specimen has been built in The Visible Human Project by National Library of Medicine. Yokota et al. (1997) have developed a novel system called three-dimensional internal structure microcopy (3D-ISM), in which bare surface images of a specimen embedded in OCT compound were serially recorded. The surface images (episcopic images) of a specimen embedded in paraffin or resin were acquired for three-dimensional reconstruction (Laan et al., 1989; Odgaard et al., 1990, 1994; Weninger et al., 1998, 2006). Although the newly cut bare surface of a frozen specimen and also paraffin block looked smooth with the naked eye, numerous tiny lumps and holes were found under a dissection microscope or a macroscope. The diffusion of reflected light by these lumps and holes markedly lowered the quality of the surface image. Various attempts have been carried out to improve the signal to noise ratio. A specimen was stained with Alcian blue (λ_{max} absorption = 620 nm) and Orange G (λ_{max} absorption = 480 nm) prior to embedding in paraffin, and the reflected light was filtered with a band pass filter, Kodak Wratten filter No. 16 (λ_{max} transmission = 500 nm) and No. 5 (λ_{max} transmission = 480 nm), respec-

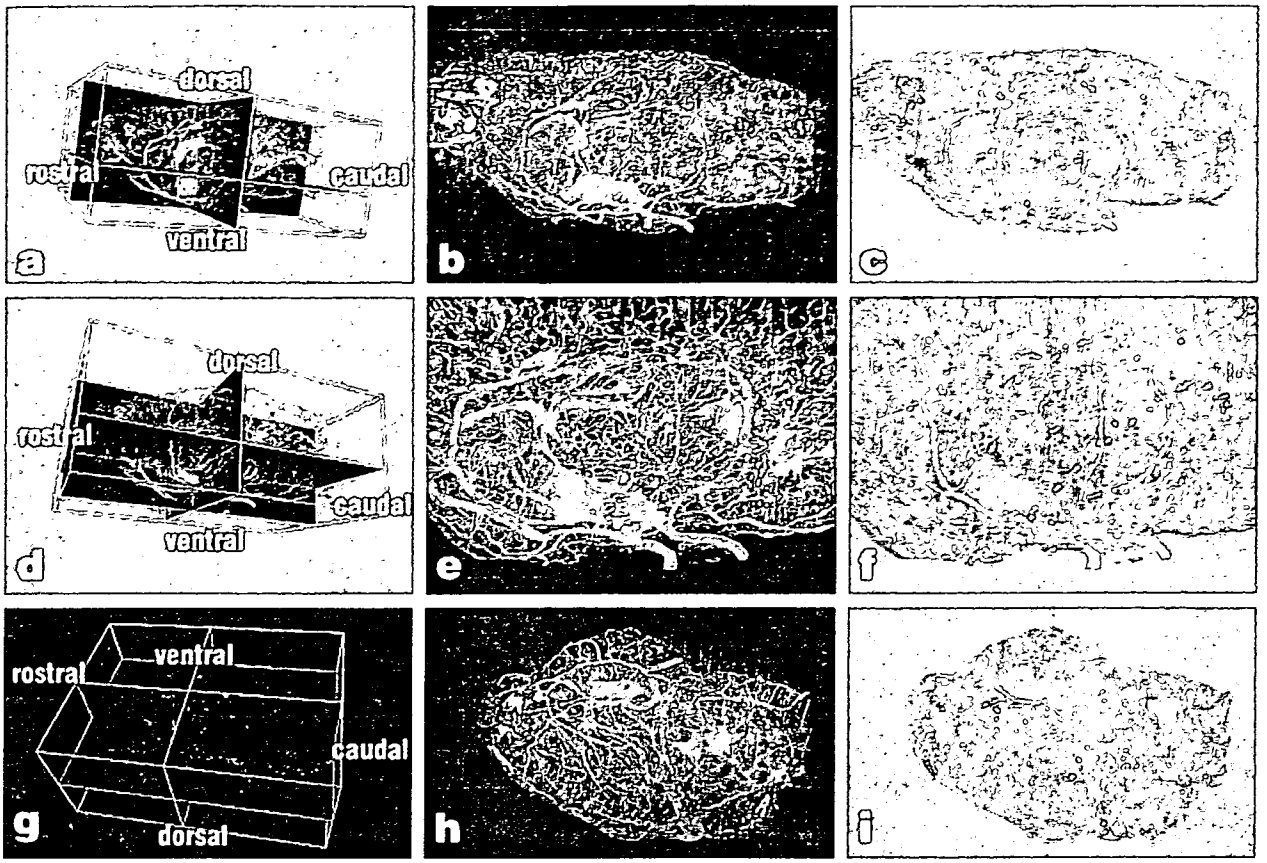

Fig. 6. Three-dimensional reconstruction of a series of serial sections from a White India ink-gelatin infused brain. A total of 1,000 horizontal sections at an interval of 5 μm were acquired from a White India ink-gelatin infused mouse brain. Alternate sections were picked up and the image size was reduced by 50%, because of the limitation of the hardware. Then, three-dimensional reconstruction was performed with an Imaris 4.2. Spatial orientation is indicated (**a**, **d**, and **g**). Volume-rendered images by the maximal intensity projection (**b**, **e**, and **h**). Volume-rendered images by the ray tracing method (**c**, **f**, and **i**). Three-dimensional distribution of blood vessels in a whole mouse brain is clearly shown from arbitrary direction and magnification. Bright white spots in the volume-rendered images by the maxima intensity projection are air bubbles in liquid paraffin (b, e, and h). On the volume-rendered images by the ray tracing method, lots of vertical fine lines along *z*-axis are seen (c, f, and i). These lines are due to stack on pixels in the CCD of the digital camera.

tively (Laan et al., 1989). The surface staining by a lead sulfide reaction was applied to a specimen infiltrated with lead acetate during dehydration (Weninger et al., 1998). Odgaard et al. (1990, 1994) used an epoxy resin containing black Araldite Coloring Paste to embed a trabecular bone and acquired surface images after placing a thin film of low-viscosity mineral oil on the block. They mentioned that the thin film of mineral oil had an enormous effect on the contrast between the white trabeculae and the black epoxy (Odgaard et al., 1990). In the present study, the newly cut surface was coated with liquid paraffin to improve the image quality of the surface. Liquid paraffin essentially has high affinity with paraffin so that tiny holes are filled with liquid paraffin and lumps are concealed in a layer of liquid paraffin. As the surface of the layer of liquid paraffin is very smooth, a sharp and clear image of the surface of the paraffin block can be taken through the layer of liquid paraffin. Jirkovská et al. (2005) adopted immersion oil between an oil immersion objective and a nondeparaffinized tissue section without cover slip to avoid the influence of mismatches in refractive index, and captured serial optical images of the nondeparaffinized tissue section by a CLSM. The immersion oil on the nondeparaffinized section improved the transparency of the section and made it possible to obtain sharp images without blurring from the section. We have used liquid paraffin instead of the immersion oil, because the immersion oil is expensive and has high viscosity. As shown in the present study, liquid paraffin improved the quality of the image of a cut surface and also increased the transparency of the paraffin block, but this caused an another problem of shadow.

The light from episcopic illumination penetrates into the paraffin and the white background of the paraffin is generated by the reflected light. The black-colored India ink-gelatin on the surface of the block does not reflect but absorbs the light, giving contrast to the white background. The India ink-gelatin in deeper vessels also absorbs the penetrated light and no light is reflected, casting a shadow on the white background. The present study showed that the length of the

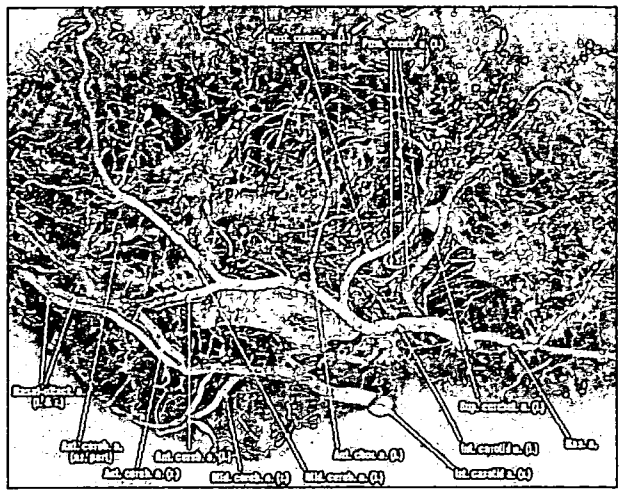

Fig. 7. Ventro-lateral view of volume-rendered image. Three-dimensionally volume-rendered image of the same specimen as in Figure 6. Major arteries are named according to the report on arterial patterns of the rat brain by Coyle (1975). Ant. cereb. a.: anterior cerebral artery. Ant. chor. a.: anterior choroidal artery. Bas. a.: basilar artery. Int. carotid. a.: internal carotid artery. Mid. cereb. a.: middle cerebral artery. Nasal-olfact. a.: nasal olfactory artery. Post. cereb. a.: posterior cerebral artery. Post. comm. a.: posterior communicating artery. Sup. cerebel. a.: superior cerebellar artery. (l.): left. (r.): right. (az. part): azygos part.

shadow in the orthogonal section image was longer than 1 mm. This indicates that the white background is generated by the reflected light from a surface layer of paraffin of over 1 mm thick and that the submerged vessels in the layer may depict the false image on the white background.

To exclude the false image of vessels, it is important to produce an image only with the light reflected at the surface of the paraffin block. Therefore, the light opaque paraffin, designated as black paraffin in the present study, was developed by dissolving the black pigment, Sudan Black B, into the melted paraffin. The black paraffin absorbs the light from episcopic illumination and no light was reflected, making the background black. The White India ink-gelatin solution, instead of the India ink-gelatin solution, was adopted to infuse vessels to make a distinct contrast against the black background by the black paraffin. Although Sudan Black B dissolved in xylene and paraffin easily penetrated into a dehydrated mouse brain and stained the brain black, the White India ink-gelatin was kept white in vessels. As a result of it, the false image of vessels was completely excluded from the surface image of black paraffin. The orthogonal section image from black paraffin indicated that the light from episcopic illumination was absorbed by the black paraffin layer of 5 μm thick and the White India ink-gelatin at 5 μm below the surface could not depict the false image. Since the surface image of the black paraffin block was produced by the black paraffin and the White India ink-gelatin within 5 μm from the surface, the *z*-axial resolution of three-dimensional image was concluded to be no longer than 5 μm.

Two types of noise, white spots of various sizes and fine straight lines parallel to the *z*-axis, were found on a three-dimensionally volume rendered image of the White India ink-gelatin infused brain. The cause of the former noise will be microbubbles in liquid paraffin. Some larger bubbles found in liquid paraffin with the naked eye can be removed prior to image acquisition, but microbubbles are difficult to recognize. However, these noises by microbubbles may be eliminated by averaging or applying AND operator to two images of the same surface acquired with a short interval, because white spots by microbubbles will move as the liquid paraffin flows. The cause of the latter will be due to stuck on pixels in the CCD of the digital camera. These noises may also be eliminated by applying an image mask prepared by acquiring a image of agarose in black paraffin to each image. However, these image processings may eliminate not only noises but also signals from the White India ink, so that three-dimensional reconstruction was performed with raw images.

Not many studies have been reported on the distribution of blood vessels in the mouse brain, though that in the rat brain has been studied by various investigators, especially in conjunction with stroke (Coyle, 1975, 1978; Coyle and Jokelainen, 1982; He et al., 2000; Koppel et al., 1982; Rieke, 1987; Rieke et al., 1981; Scremin, 2004; Ward et al., 1990). The rat cerebral vascular system is widely reviewed and appears in a textbook (Scremin, 2004). The methodologies used in the past studies were scanning electron microscopical observation of corrosion casts of the vasculature and light microscopical observation of brain sections injected with a mixture containing India ink. Recently, we have developed a novel method to examine three-dimensional distribution of vascular nets with CLSM (Hashimoto et al., 1998a,b, 1999). In this method, a fluorochrome-labeled gelatin was injected into the vascular system and a thick slice of an organ was observed with a CLSM to reconstruct a three-dimensional image of vascular networks from optical serial sections. By preparing two types of fluorochrome-labeled gelatin with different fluorescence spectrum, arterial and venous systems were broadly distinguished. These methods are useful and effective for investigating vascular nets in a small region, but are not suitable for a larger specimen, such as a whole brain. Although the combination of μCT, synchrotron radiation μCT and scanning electron microscopic imaging of corrosion casts may be feasible for three-dimensional observation of vascular networks in a whole brain (Heinzer et al., 2006), the μCT has not been generally available yet and, furthermore, the availability of a synchrotron is quite limited. On the contrary, the present method is very simple and the equipment used is common and inexpensive.

While a three-dimensional image by μCT is reconstructed from multiple angular views using a tomographic reconstruction algorithm, such as a modified Feldkamp's filtered back projection algorithm (Bentley et al., 2002), a three-dimensional image in the present method is reconstructed by heaping up direct images of serial cross sections. Therefore, the present method may provide a reference model of three-dimensional distribution of vascular networks in a mouse brain, to reconfirm its three-dimensional image taken by μCT.

In conclusion, we propose a novel method for three-dimensional observation of vascular networks in a whole mouse brain, which is summarized as follows.

(1) Under deep anesthesia, a mouse is infused with a fixative and the White India ink-gelatin solution. (2) After the White India ink-gelatin is made to gel on ice, the brain is removed and further fixed. (3) The brain is embedded in agarose, dehydrated with a graded series of ethanol and further embedded in paraffin containing Sudan Black B through xylene containing Sudan Black B. (4) A series of serial images is acquired from each newly sliced surface of the paraffin block after coating with liquid paraffin. (5) Three-dimensional image is reconstructed from the serial images with a volume-rendering software. A proper understanding of the vascular system in a normal brain of the mouse is indispensable to reveal the development of the vascular system in the brain of normal and genetically manipulated mice, genetic control of the development of the vascular system and vascular alterations in pathological situation, such as stroke, ischemia, and neurodegenerative disease. The present method will provide fundamental information on the vascular system in a whole mouse brain.

REFERENCES

Bentley MD, Ortiz MC, Ritman EL, Romero JC. 2002. The use of microcomputed tomography to study microvasculature in small rodents. Am J Physiol Regulat Integr Comp Physiol 282:R1267–R1279.

Coyle P. 1975. Arterial pattern of the rat rhinencephalon and related structures. Exp Neurol 49:671–690.

Coyle P. 1978. Spatial features of the rat hippocampal vascular system. Exp Neurol 58:549–561.

Coyle P, Jokelainen PT. 1982. Dorsal cerebral arterial collaterals of the rat. Anat Rec 203:397–404.

Hashimoto H, Ishikawa H, Kusakabe M. 1998a. Simultaneous observation of capillary nets and tenascin in intestinal villi. Anat Rec 250:488–492.

Hashimoto H, Ishikawa H, Kusakabe M. 1998b. Three-dimensional investigation of vascular nets by fluorochrome-labeled angiography. Microvasc Res 55:179–183.

Hashimoto H, Ishikawa H, Kusakabe M. 1999. Preparation of whole mounts and thick sections for confocal microscopy. Methods Enzymol 307:84–107.

He Z, Yang SH, Naritomi H, Yamawaki T, Liu Q, King MA, Day AL, Simpkins JW. 2000. Definition of the anterior choroidal artery territory in rats using intraluminal occluding technique. J Neurol Sci 182:16–28.

Heinzer S, Krucker T, Stampanoni M, Abela R, Meyer EP, Schuler A, Schneider P, Müller R. 2006. Hierarchical microimaging for multiscale analysis of large vascular networks. Neuroimage 32:626–636.

Jirkovská M, Náprstková I, Janáícek J, Kuicera T, Macáisek J, Karen P, Kubínová L. 2005. Three-dimensional reconstructions from non-deparaffinized tissue sections. Anat Embryol 210:163–173.

Jorgensen SM, Demirkaya O, Ritman EL. 1998. Three-dimensional imaging of vasculature and parenchyma in intact rodent organs with X-ray micro-CT. Am J Physiol 275:H1103–H1114.

Kimura J, Tsukise A, Yokota H, Nambo Y, Higuchi T. 2001. The application of three-dimensional internal structure microscopy in the observation of mare ovary. Anat Histol Embryol 30:309–312.

Koppel H, Lewis PD, Wigglesworth JS. 1982. A study of the vascular supply to the external granular layer of the postnatal rat cerebellum. J Anat 134:73–84.

Krucker T, Lang A, Meyer EP. 2006. New polyurethane-based material for vascular corrosion casting with improved physical and imaging characteristics. Microsc Res Tech 69:138–147.

Laan AC, Lamers WH, Huijsmans DP, Kortschot AT, Smith J, Strackee J, Los JA. 1989. Deformation-corrected computer-aided three-dimensional reconstruction of immunohistochemically stained organs: Application to the rat heart during early organogenesis. Anat Rec 224:443–457.

Odgaard A, Andersen K, Melsen F, Gundersen HJG. 1990. A direct method for fast three-dimensional serial reconstruction. J Microsc 159:335–342.

Odgaard A, Andersen K, Ullerup R, Frich LH, Melsen F. 1994. Three-dimensional reconstruction of entire vertebral bodies. Bone 15:335–342.

Plouraboué F, Cloetens P, Fonta C, Steyer A, Lauwers F, Marc-vergnes JP. 2004. X-ray high-resolution vascular network imaging. J Microsc 215:139–148.

Ricke GK. 1987. Thalamic arterial pattern: An endocast and scanning electron microscopic study in normaotensive male rats. Am J Anat 178:45–54.

Ricke GK, Bowers DE, Penn P. 1981. Vascular supply pattern to rat caudatoputamen and globus pallidus: Scanning electron microscopic study of vascular endocasts of stroke-prone vessels. Stroke 12:840–847.

Scremin OU. 2004. Cerebral vascular system. In: Paxinos G, editor. The rat nervous system, 3rd ed. San Diego, CA: Academic Press. pp. 1167–1202.

Ward R, Collins RL, Taguay G, Miceli D. 1990. A quantitative study of cerebrovascular variation in inbred mice. J Anat 173:87–95.

Weninger WJ, Meng S, Streicher J, Müller GB. 1998. A new episcopic method for rapid 3-D reconstruction: Applications in anatomy and embryology. Anat Embryol 197:341–348.

Weninger WJ, Geyer SH, Mohum TJ, Rasskin-Gutman D, Matsui T, Ribeiro I, Costa LF, Izpisúa-Belmonte JC, Müller GB. 2006. High-resolution episcopic microscopy: A rapid technique for high detailed 3D analysis of gene activity in the context of tissue architecture and morphology. Anat Embryol 211:213–221.

Yokota H, Kudoh K, Sato K, Higuchi T. 1997. Development of a 3-dimensional internal structure microscope (3D-ism) for the observation to biological organism. In: Bailey GW, editor. Proceedings of Microscopy and Microanalysis, Vol. 3. New York: Microscopy Society of America. pp. 243–244.

Development of the Mucosal Vascular System in the Distal Colon of the Fetal Mouse

TAKAYASU ITO,[1] SATOSHI OHI,[1] TOSHIAKI TACHIBANA,[1] MASASHI TAKAHARA,[1] TETSUYA HIRABAYASHI,[1] HIROSHI ISHIKAWA,[1,2] MORIAKI KUSAKABE,[3,4,5] AND HISASHI HASHIMOTO[1]*

[1]Department of Anatomy, The Jikei University School of Medicine, Minato-ku, Tokyo, Japan

[2]Laboratory of Regenerative Medical Science, The Nippon Dental University School of Life Dentistry at Tokyo Chiyoda-ku, Tokyo, Japan

[3]Research Center for Food Safety, Graduate School of Agricultural and Life Sciences, The University of Tokyo, Bunkyo-ku, Tokyo, Japan

[4]Matrix Cell Research Institute, Inc., Ibaraki, Japan

[5]Institute for Animal Reproduction (IAR), Experimental Animal Research Center, Kasumigaura, Ibaraki, Japan

ABSTRACT

The formation of the crypt in the distal colon of the mouse was investigated in association with the development of vascular networks. For histological observation, 1-μm cross-sections were made from the distal colon of fetal mice in 13 to 18 days of gestation. Three-dimensional distributions of vascular networks in the organ were observed after perfusing fetuses with rhodamine isothiocyanate-labeled gelatin and immunostaining for laminin to examine the boundary between the epithelium and the mesenchyme. At 13 days of gestation, the distal colon and its epithelium formed a cylindrical tube and a loose primary plexus of vessels was built in the mesenchyme. In the distal colon of 15 days of gestation, the caudal portion began to form the crypt and the vascular plexus built up from a few layers was situated apart from the boundary between the epithelium and the mesenchyme. As the development proceeded, the formation of the crypt occurred in the caudorostral direction. The developing crypt advanced into the vascular plexus, so that a few vessels situated in the mesenchyme between crypts. As the crypt elongated, these vessels formed a small plexus situated perpendicular to the primary plexus, while the primary plexus became monolayered and loosened. The new plexus was composed of ascending vessels and traversing ones, but the regular honeycomb-like plexuses around openings of crypts have not established yet even in 18 days of gestation. The vascular system as well as the crypt in the distal colon will take further a few postnatal weeks to be completed. Anat Rec, 291:65–73, 2007. © 2007 Wiley-Liss, Inc.

Key words: mouse; distal colon; crypt; fetus; vascular networks; three-dimensional reconstruction

Grant sponsor: Japan Society for the Promotion of Science (JSPS); Grant number: 18390355.

*Correspondence to: Hisashi Hashimoto, Department of Anatomy, The Jikei University School of Medicine, 3-25-8 Nishishinbashi, Minato-ku, Tokyo, 105-8461, Japan. Fax: 81-3-3433-2065. E-mail: hashimoto.anat@jikei.ac.jp

Received 10 April 2007; Accepted 5 October 2007

DOI 10.1002/ar.20621

Published online in Wiley InterScience (www.interscience.wiley.com).

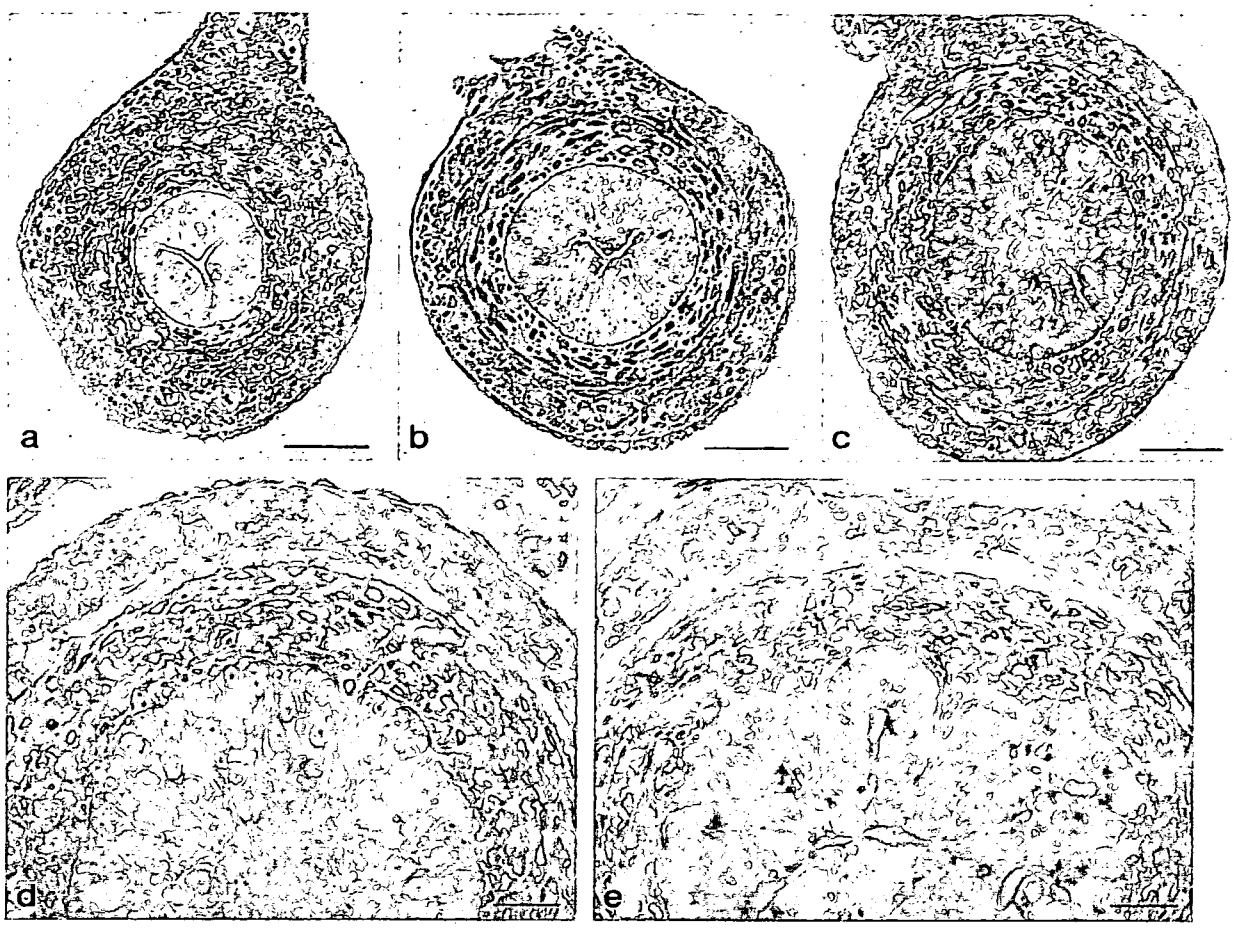

Fig. 1. Cross-sections of the distal colon in day 13 to 15 fetal mice. **a:** Day 13. **b:** Day 14. **c–e:** Day 15, a rostral portion (c,d) and a caudal portion (e). The epithelium of the distal colon in 13 and 14 days of gestation is a cylindrical tube with a slit like lumen (a,b). Circularly and longitudinally arranged cells, the future circular and longitudinal muscle layers, appear in the mesenchyme of day 14 distal colon (b). The epithelium in the rostral portion is still cylindrical, but the formation of the crypt begins in the caudal portion in the day 15 distal colon (c–e). Scale bar = 500 μm in a–c, 200 μm in d,e.

The colonic microcirculation system in the mouse (Ravnic et al., 2007) has a distinctive characteristic as well as in the other mammals such as rats, guinea pigs, and humans (Browning and Gannon, 1986; Aharinejad et al., 1992; Araki et al., 1996; Skinner and O'Brien, 1996). Arterioles ascending from the submucosal plexus ramify and form the polygonal subepithelial plexus, and venules descend from the subepithelial plexus and drain into the submucosal plexus. The subepithelial plexus is composed of uniform polygonal networks of capillaries that surround the orifice of the crypt. Therefore, the colonic microcirculation system has a close relationships with the crypt. We have a few reports on the development of the colon in the mouse (Chen and Kataoka, 1991; Ménard et al., 1994) and the rat (Eastwood and Trier, 1973; Helander, 1973; Brackett and Townsend, 1980), but no report on the development of the colonic microcirculation system in any mammal. It is not clear yet how these microcirculation system is constructed.

Recently, we have developed a novel method, the fluorochrome-labeled gelatin method, to visualize three-dimensional distribution of vascular nets with a confocal laser scanning microscope. A fluorochrome-gelatin solution never solidifies while it is warmed, so that this solution is easy to handle and has no time limit to inject. Therefore, this method is easily applicable and especially suitable to an experiment on an embryo and fetus. With this method, we have reported a three-dimensional analysis of vascular nets in the pituitary gland and the small intestine of the mouse during the fetal development (Hashimoto et al., 1998, 1999b).

In the present study, we have applied this fluorochrome-labeled gelatin method to investigate the development of microcirculation system in the fetal distal colon of the mouse. Much attention was focused on the interrelationship between the initial formation of the crypt and distribution of vascular nets.

MATERIALS AND METHODS

Animals

The ICR strain of mice were obtained from CLEA Japan, Inc. (Tokyo, Japan), maintained in our laboratory (Department of Anatomy, Jikei University School of

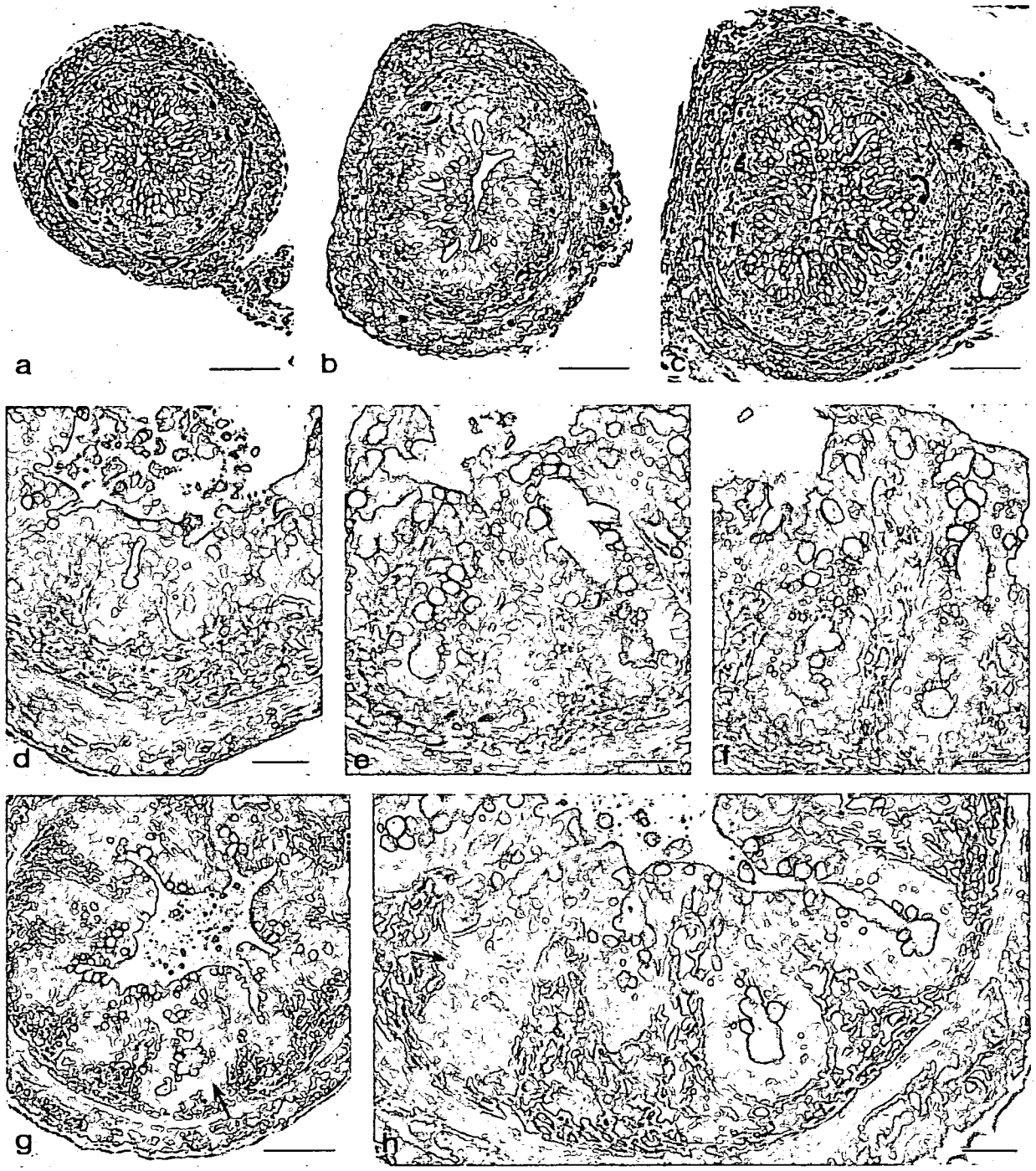

Fig. 2. Cross-sections of the distal colon in day 16 (a–c), 17 (d–f), and 18 (g,h) fetal mice. a–c: A rostral portion (a), a middle portion (b), and a caudal portion (c) in a distal colon of day 16 fetal mouse. d–f: A rostral portion (d), a middle portion (e), and a caudal portion (f) in a distal colon of day 17 fetal mouse. The formation of the crypt is more advanced in the caudal portion than in the rostral portion (a–f). The branching of the crypt is found in the day 18 distal colon (arrows in g,h). Scale bar = 500 μm in a–c,g, 200 μm in d–f,h.

Medicine) as a closed colony and housed in a temperature-controlled (22°C) and light-controlled (14 hr light/day) room with free access to tap water and diet (CE-2, CLEA Japan, Inc.). In calculating the embryonic age, the morning when a copulation plug was found after overnight mating was designated as day 0. All experiments were performed under the Guideline on Animal Experimentation of the Jikei University.

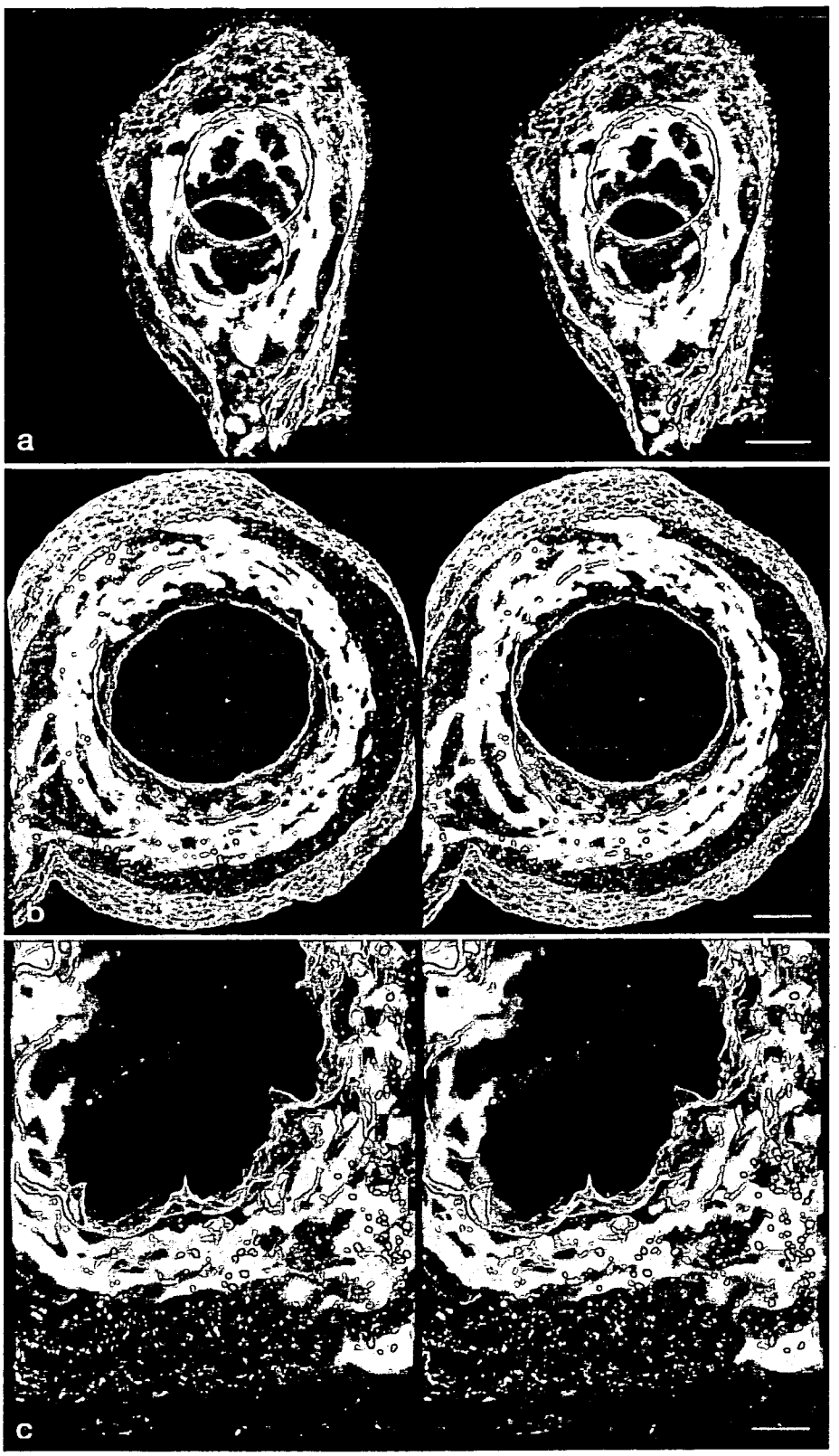

Figure 3.

Vascular Cast With Rhodamine isothiocyanate (RITC)-Labeled Gelatin

Gelatin (approximately 225 Bloom, No. G9382, Sigma Co., St. Louis, MO) was labeled with RITC (R1755, Sigma-Aldrich Japan K.K., Tokyo, Japan) as mentioned previously (Hashimoto et al., 1998, 1999a,b). Before perfusion, the rhodamine isothiocyanate (RITC)-labeled gelatin solution was dissolved in a hot (approximately 60°C) water bath, diluted with 0.01 M phosphate buffered saline (PBS, pH 7.4) to make a final concentration of gelatin of approximately 10%, and loaded into a 1-ml syringe connected with a glass needle by means of a plastic tube. The syringe with plastic tube and needle was kept at 37°C in a warm-water bath until use.

Pregnant mice of 13 to 19 days of gestation were killed by ether inhalation, and the pups, along with their intact fetal membranes, were removed immediately and kept in an ice-cold PBS. Each fetus was transferred to warm (37°C) PBS, and fetal membranes were removed to expose the umbilical cord. Under a dissection microscope, the glass needle was inserted into the umbilical vein, and the umbilical artery was severed. The insertion of the needle induced contractions of the vein at the inserted point and the blood flow was almost blocked. The RITC-labeled gelatin solution was, then, slowly injected into the vein, and blood flowed from the umbilical artery. The injection rate of the gelatin solution was initially adjusted to the flow rate of the blood stream just before it was blocked and then gradually slowed down. Meticulous care was taken not to swell the vein by injecting too much gelatin solution. The perfusion continued until no more red blood cells flowed from the artery. After perfusion, the fetus was immersed immediately in a chilled fixative, which consisted of 0.5% paraformaldehyde and 15% (vol/vol) of a saturated picric acid solution in 0.1M sodium phosphate buffer (pH 7.0). After solidification of the RITC-labeled gelatin, the distal colon, which was attached to the posterior abdominal wall with a short mesocolon, was removed and further fixed in the same fixative at 4°C for more than 1 day.

Histological Observation

The distal colon was further fixed in 4% paraformaldehyde in 0.1 M sodium phosphate buffer (SPB, pH 7.2) for 1 day or more at room temperature. After rinsing with SPB, the organ was transversely cut into small pieces, dehydrated with a graded series of ethanol, immersed in a hydrophilic resin mixture (2-hydroxypropyl methacrylate: triethylene glycol dimethacrylate: 2-butoxyethanol = 7:0.25:1) containing 0.05%(w/v) of benzoin methyl ether, and embedded vertically in the resin mixture (modified from Franklin, 1982). The resin mixture was cured under ultraviolet irradiation for 1 hr at room temperature. The resin block was sectioned at a thickness of 1 μm with a MT-2B ultramicrotome and a glass knife and a cross-section of the organ was obtained. Each section was stained with methylene blue and basic fuchsine (Bennett et al., 1976).

Immunostaining Methods

The distal colon was then rinsed with cold SPB (pH 7.2) several times and transferred to PBS containing 5% sucrose, PBS containing 10% sucrose, and finally PBS containing 20% sucrose and 10% glycerin, 3 hr each at 4°C. The organ was rapidly frozen on a freezing stage (K400, Microm Laborgeräte GmbH, Walldorf, Germany) attached to a sliding microtome (HM400R, Microm Laborgeräte GmbH) and sectioned at a thickness of 150 μm. The sections were rinsed with chilled PBS and pretreated with a 3% aqueous solution of sodium deoxycholate overnight at 4°C. After rinsing with chilled distilled water, the sections were immunostained for laminin. The pretreated sections were rinsed with chilled PBS, incubated with 10% normal goat serum overnight at 4°C, and then incubated with rabbit anti-mouse laminin antibody (AT-2404, E.Y. Laboratories, Inc., San Mateo, CA) diluted 1:500 with PBS containing 1% bovine serum albumin and 0.01% sodium azide for 1 day at 4°C. The sections were then rinsed repeatedly with chilled PBS for several hours, incubated with goat anti-rabbit IgG antibody conjugated with fluorescein isothiocyanate (FITC; #55662, Cappel, Organon Teknika Corp., Durham, NC) diluted 1:200 for 1 day at 4°C, rinsed again with chilled PBS and observed with a laser scanning microscope.

For controls, either the primary antibody was eliminated, or normal rabbit serum diluted 1:500 was used in place of the primary antibody. This control serum was found not to contain the specific antibody. The mouse laminin antibody reacted with both A and B chains on an immunoblot. The immunoreaction of this antibody (1:500) was absorbed completely after incubation with 100 μg/ml purified mouse laminin (no. 40232, CR Inc., Bedford, MA).

Observations

The thick sections were mounted with 0.05M Tris-HCl buffered saline (pH 8.0) containing 90% (vol/vol) of non-fluorescent glycerin and 10 mg/ml of 1,4-diazabicyclo-[2,2,2] octane (DABCO, Wako Pure Chemical Corp., Osaka, Japan), and observed with a Carl Zeiss LSM-510 confocal laser scanning microscope (Jena, Germany). The double-stained sections were stimulated with both argon laser at 488 nm and He-Ne laser at 543 nm. The emitted fluorescence was divided with a HFT 488/543 dichronic beam splitter. The fluorescence of FITC was obtained through a band pass filter of 505–530 nm and that of RITC was observed through a long pass filter at 560 nm. Serial images of the optical sections were obtained at an interval of half of the full width at half-

Fig. 3. **a–c:** Stereo pair images of vascular nets (red) and laminin (green) in the distal colon of day 13 (a) and 15 (b,c) fetal mice. b: A rostral portion. c: A caudal portion. The vascular plexus is composed of mono-layered vessels in the day 13 distal colon (a) and of a few layered vessels in day 15 (b). In the caudal portion of the day 15 distal colon, the boundary between the epithelium and the mesenchyme is concaved and convexed, but the vascular plexus is situated apart from the boundary (c). Three-dimensional stereo pair images were reconstructed from 57 (a), 56 (b), and 59 (c) images taken at an interval of 2 (a), 1.5 (b), and 1 (c) μm, respectively. Scale bar = 50 μm in a,b, 25 μm in c.

Figure 4.

maximum value calculated from the parameters of the optical system applied. For three-dimensional observation, stereo pair images were generated by the pixel-shifting algorhythm with maximum intensity projection at right–left angle of 6° by using the LSM software prepared by Carl Zeiss Co.

RESULTS

Histological Observation

At 13 days of gestation, the cross-section of the distal colon consisted of a cylindrical epithelial tube and a surrounding thick layer of mesenchyme (Fig. 1a). The epithelial cell was cuboidal or cylindrical and its nucleus was arranged in two or three layers except where the slit-like lumen extended (Fig. 1a). The lumen sometimes ramified resulting in a narrow triangular appearance (Fig. 1a). At 14 days of gestation, the epithelial cells were compressed and became slender and the slit-like lumen extended between banks of the epithelial cells (Fig. 1b). In the mesenchyme, the future circular and longitudinal muscle layers appeared as a condensation of spindle-shaped cells (Fig. 1b). At 15 days of gestation, the epithelial cells became multilayered and the boundary between the epithelium and the mesenchyme partly became concaved and convexed in the rostral portion of the distal colon (Fig. 1c,d). The lumen further ramified and extended between the epithelial cells (Fig. 1c,d). In the caudal portion of the distal colon, the tip of the lumen expanded and a monolayered cylindrical cells lining the expanded tip of the lumen began to bulge into the surrounding mesenchyme layer (Fig. 1e). This was the first appearance of the crypt. In a cross-section of the distal colon from 16 days of gestation, a few slits appeared between the epithelial cells in the bank and new origins of the crypt were formed (Fig. 2a–c). The epithelium lining the crypt became monolayered, whereas that between the crypts stayed multilayered (Fig. 2a–c). Serial cross-sections of the distal colon from 16 days of gestation revealed that the crypt formation anticipated in the caudal portion of the distal colon. The epithelium in the rostral portion of the distal colon was still principally multilayered, and monolayered epithelial cells were cylindrical, whereas those in the caudal portion became cuboidal and began to bulge into the mesenchyme layer (Fig. 2a–c). At 17 days of gestation, the crypt became deeper and the surface epithelium located between crypts was almost monolayered (Fig. 2d–f). In the epithelium lining of the crypt, the goblet cells appeared. The crypt was more developed and more goblet cells were observed in the middle to caudal portion than in the rostral portion of it (Fig. 2d–f). In the distal colon of 18 days of gestation, the crypt extended nearly to the circular muscle layer and the lumen at the base of the crypt dilated (Fig. 2g,h). Some crypts began to ramify (Fig. 2g). The goblet cell became prominent in both the cryptal and surface epithelium (Fig. 2g,h). The cryptal epithelial cells at the base of the crypt became cuboidal, whereas those at the middle and upper portion of the crypt were cylindrical, including the goblet cell (Fig. 2h). The surface epithelial cells were also cylindrical, and the goblet cell intervened between them (Fig. 2h).

Development of Capillary Networks

The vascular system in the fetal distal colon was well filled with RITC-labeled gelatin, and a whole vascular network in the organ was three-dimensionally observed. Three-dimensional images of laminin clearly indicated the boundary between the epithelium and the mesenchyme, including the crypt. Therefore, developmental changes in the spatial relationship between the crypt and the vascular system were distinctively shown.

A loose primary vascular plexus was found in the mesenchyme surrounding the tubular epithelium in the distal colon of 13 days of gestation (Fig. 3a). The primary vascular plexus roughly invested the tubular epithelium (Fig. 3a). The primary vascular plexus became multilayered as the development proceeded. The vascular networks of 15 days of gestation were built up from a few layers of vascular plexus in the mesenchyme and some vessels running in the future muscular layer, to which some tributaries from large vessels running in the mesentery and subserosal layer connected (Fig. 3b,c). These vessels were situated slightly apart from the basal lamina of the epithelium, even in the caudal portion where the basal lamina had become concaved and convexed (Fig. 3c). At 16 days of gestation, the vascular plexus had slightly become loosened (Fig. 4a). The developing crypt advanced into the vascular plexus, so that a few vessels situated in the mesenchyme between crypts (Fig. 4b). The vessels around the crypt run the neighborhood of the basal lamina but never attached to it (Fig. 4b). As the development of the crypt advanced, vessels located in the mesenchyme between crypts formed a small plexus situated perpendicular to the primary plexus, whereas the primary plexus became monolayered and loosened (Figs. 4c, 5). The new plexus was composed of ascending vessels and traversing ones, but the regular honeycomb-like plexus around openings of crypts have not established yet even in 18 days of gestation (Fig. 5).

DISCUSSION

In the present study, we have shown that the formation of the crypt began at day 15 of gestation and advanced in a caudorostral direction in the distal colon. The caudal portion of the distal colon preceded the rostral portion of it in the development of the crypt and the cytodifferentiation of the epithelium. Before the formation of the crypt, the distal colon and its epithelium was a cylindrical tube, and a loose monolayered and then multilayered plexus of vessels, the primary plexus, was built in the mesenchyme layer. As the simplified epithelium began the downgrowth

Fig. 4. Stereo pair images of vascular nets (red) and laminin (green) in the distal colon of day 16 (**a,b**) and 17 (**c**) fetal mice. The crypt indicated by laminin advances to and into the vascular plexus (a–c) and vessels in the inner layer of the plexus locate in the mesenchyme between crypts and form a small plexus (b,c). Vessels in the outer layer of the plexus keep their location and distribution (c). Three dimensional stereo pair images were reconstructed from 38 (a), 41 (b), and 52 (c) images taken at an interval of 1.5 (a), 0.76 (b), and 1 (c) μm, respectively. Scale bar = 50 μm in a, 25 μm in b,c.

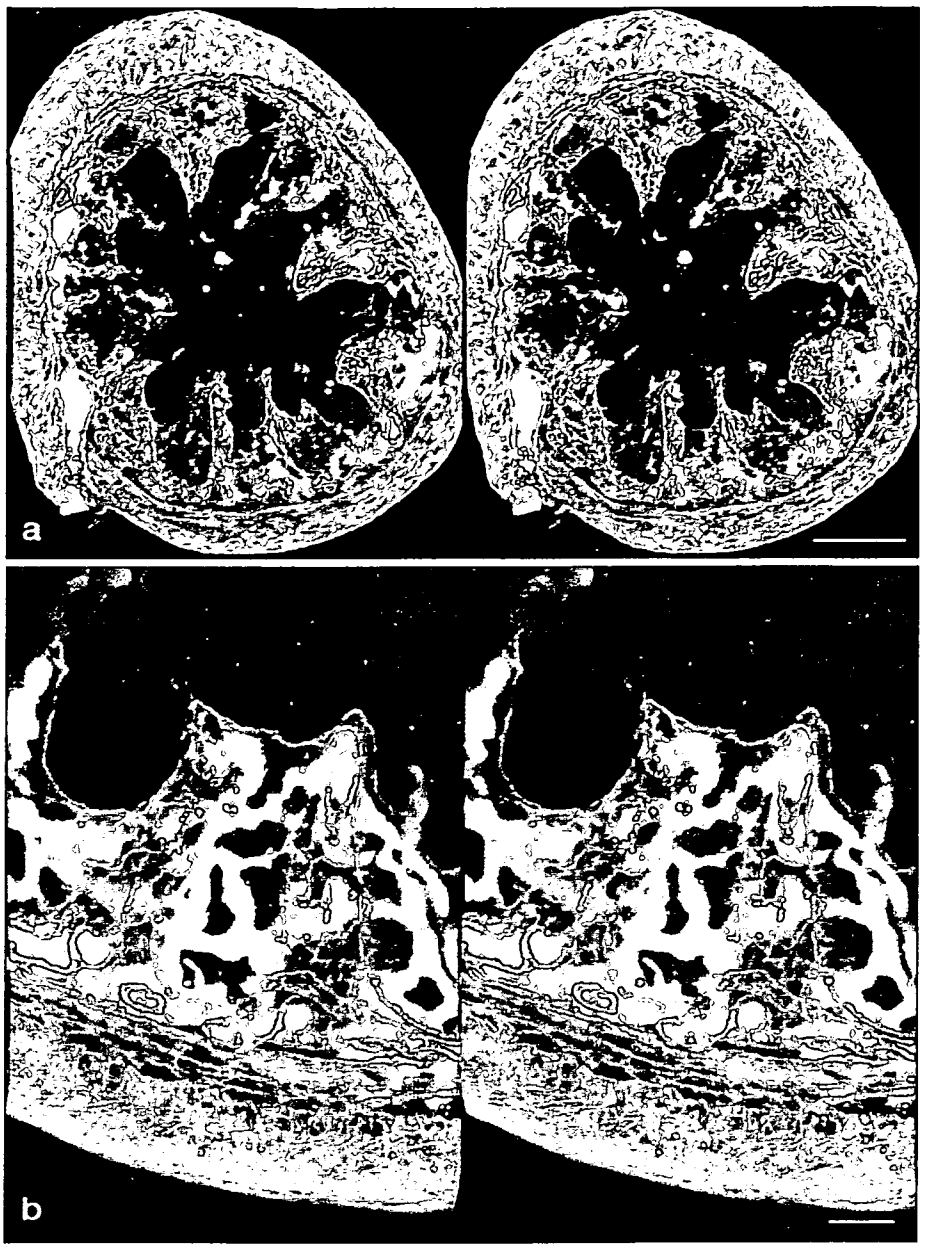

Fig. 5. Stereo pair images of vascular nets (red) and laminin (green) in the distal colon of day 18 fetal mice. **a:** The crypt elongates and bifurcates in places. **b:** The small plexus in the mesenchyme between crypts is composed of ascending vessels and traversing ones. The distribution of vessels in the outer layer of the plexus is unchanged (b). Three-dimensional stereo pair images were reconstructed from 57 (a) and 46 (b) images taken at an interval of 2.3 (a) and 0.8 (b) μm, respectively. Scale bar = 50 μm in a, 25 μm in b.

into the mesenchyme to form the crypt, the inner layer of the primary plexus was left or incorporated in the mesenchyme between crypts, whereas the outer circular layer of it was located inside of the muscular layer. The inner layer of the primary plexus in the mesenchyme between crypts formed the secondary plexus of vessels located perpendicular to the primary plexus. A vessel in the secondary plexus traversed the mesenchyme beneath the surface epithelium in places.

The present study indicates that the formation of the crypt in the distal colon begins in the caudal portion and proceeds toward the rostral portion (caudorostral sequence of differentiation). According to Gordon and Hermiston (1994), the gut endoderm undergoes rapid remodeling from embryonic day (E) 15 to E19 as a proximal-to-distal wave of cytodifferentiation converts it from a pseudostratified epithelium to a monolayer of columnar epithelial cells. However, this description is applica-

ble to the small intestine but not to the large intestine. Asynchronous development of the colonic epithelium in the mouse was reported by Chen and Kataoka (1991), but they did not notice the direction of the developmental gradient. Ménard et al. (1994) stated that the development of the mouse colonic crypts is asynchronous in the proximal and distal segments and that distal colonic crypts are already well defined at day 2 after birth, while they are barely identifiable in the proximal segment. Therefore, as stated by Asari et al. (1986), the wave of maturation of the mucosa in the small intestine begins at the duodenum and proceeds toward the ileum in the small intestine, whereas it subsequently proceeds from the rectum toward the cecum in the large intestine, with maturation zones finally joining and near the ileocecal area in fetal or early neonatal period.

Comparing the development of the vascular system in the distal colon with that in the small intestine by Hashimoto et al. (1999b), some remarkable differences were noticed. The initial formation of the primary vascular plexus in the distal colon was comparable to that in the small intestine. Thereafter, in the small intestine, a few vessels from the dense primary plexus projected into the ridges of the mesenchyme and attached to the epithelial basement membrane, indicating the initial formation of the capillary loop in villi. No vessels approached nor attached to the epithelial basement membrane in the large intestine before the initiation of the crypt formation. While the top of the capillary loop was always placed at the top of the mesenchyme in the villus throughout its development in the small intestine, a small plexus was formed in the mesenchyme between crypts and only a few vessels in the plexus traversed the mesenchyme beneath the surface epithelium in places in the distal colon.

The vascular system as well as the crypt in the distal colon has not been completed in the fetal period. At day 18 of gestation, ridges of the mesenchyme between crypts, which were indicated by the immunolocalization of laminin, had irregular heights and were waved. It will take a further few postnatal weeks to be established, as stated by Ménard et al. (1994), that crypts further develop during the postnatal days, and by 16 days, they have elongated and increased in number. During a few postnatal weeks, the rearrangement of the mucosal vascular system will occur with the maturation of the crypt.

Although the developmental change of the vascular system is closely bound up with the histogenesis of an organ, we have few reports on it because of its difficulty in investigation. As stated earlier (Hashimoto et al., 1998; 1999a,b), the fluorochrome-labeled gelatin method used in the present study is easily applicable to fetuses. The vascular nets along with the other substance, such as laminin in this study, are three-dimensionally observable without any difficulty. Therefore, the fluorochrome-labeled gelatin method will afford new insight to the investigation of the vascular development during organogenesis in vivo.

LITERATURE CITED

Aharinejad S, Gangler P, Hagen D, Firbas W. 1992. Studies on the microvascularization of the digestive tract by scanning electron microscopy of vascular corrosion casts. I. Large intestine in rats and guinea pigs. Acta Anat 144:278–283.

Araki K, Furuya Y, Kobayashi M, Matsuura K, Ogata T, Isozaki H. 1996. Comparison of mucosal microvasculature between the proximal and distal human colon. J Electron Microsc 45:202–206.

Asari M, Kashiwazaki N, Kawaguchi N, Fukaya K, Kano Y. 1986. Developmental changes in the inner surface structure of the bovine large intestine. Acta Anat 127:137–141.

Bennett HS, Wyrick AD, Lee SW, McNeil JH. 1976. Science and art in preparing tissues embedded in plastic for light microscopy, with special reference to glycol methacrylate, glass knives and simple stains. Stain Technol 51:71–97.

Brackett KA, Townsend SF. 1980. Organogenesis of the colon in rats. J Morphol 163:191–201.

Browning J, Gannon B. 1986. Mucosal microvascular organization of the rat colon. Acta Anat 126:73–77.

Chen ZJ, Kataoka K. 1991. Histogenesis of the mucosa of the descending colon in mouse fetuses. Arch Histol Cytol 54:221–232.

Eastwood GL, Trier JS. 1973. Epithelial cell proliferation during organogenesis of rat colon. Anat Rec 179:303–310.

Franklin RM. 1982. Pre-embedding staining for immunohistochemistry at the light microscopic level. In: Bullock GR, Petrusz P, editors. Techniques in immunocytochemistry. Vol. 1. London: Academic Press. p 251–268.

Gordon JI, Hermiston ML. 1994. Differentiation and self-renewal in the mouse gastrointestinal epithelium. Curr Opin Cell Biol 6:795–803.

Hashimoto H, Ishikawa H, Kusakabe M. 1998. Three-dimensional analysis of the developing pituitary gland in the mouse. Dev Dyn 212:157–166.

Hashimoto H, Ishikawa H, Kusakabe M. 1999a. Preparation of whole mounts and thick sections for confocal microscopy. In: Methods in enzymology. Vol. 307. Confocal microscopy. New York: Academic Press. p 84–107.

Hashimoto H, Ishikawa H, Kusakabe M. 1999b. Development of vascular networks during the morphogenesis of intestinal villi in the fetal mouse. Acta Anat Nippon 74:567–576.

Helander HF. 1973. Morphological studies on the development of the rat colonic mucosa. Acta Anat 85:153–176.

Ménard D, Dagenais P, Calvert R. 1994. Morphological changes and cellular proliferation in mouse colon during fetal and postnatal development. Anat Rec 238:349–359.

Ravnic DJ, Konerding MA, Tsuda A, Huss HT, Wolloscheck T, Pratt JP, Mentzer SJ. 2007. Structural adaptations in the murine colon microcirculation associated with hapten-induced inflammation. Gut 56:518–523.

Skinner SA, O'Brien PE. 1996. The microvascular structure of the normal colon in rats and humans. J Surg Res 61:482–490.

STEM CELLS®

Microarray Analyses Support a Role for Nurr1 in Resistance to Oxidative Stress and Neuronal Differentiation in Neural Stem Cells

Kyle M. Sousa, Helena Mira, Anita C. Hall, Lottie Jansson-Sjöstrand, Moriaki Kusakabe and Ernest Arenas

Stem Cells 2007;25;511-519; originally published online Oct 12, 2006;
DOI: 10.1634/stemcells.2006-0238